Article

Metal "Capture" by a Heterotrimetalloligand, Heterometallic d–d Interactions, and Unexpected Iron-to-Platinum Silyl Ligand Migration: a Combined Experimental and Theoretical Study

Walter Schuh, Pierre Braunstein, Marc Bnard, Marie-Madeleine Rohmer, and Richard Welter

J. Am. Chem. Soc., **2005**, 127 (29), 10250-10258• DOI: 10.1021/ja051389z • Publication Date (Web): 01 July 2005

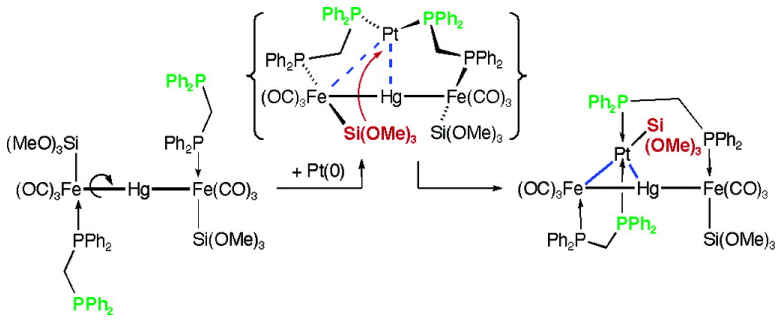

More About This Article

Additional resources and features associated with this article are available within the HTML version:

- Supporting Information
- Links to the 2 articles that cite this article, as of the time of this article download
- Access to high resolution figures
- Links to articles and content related to this article
- Copyright permission to reproduce figures and/or text from this article

View the Full Text HTML

J|A|C|S
ARTICLES
Published on Web 07/01/2005

Metal "Capture" by a Heterotrimetalloligand, Heterometallic $d^{10}-d^{10}$ Interactions, and Unexpected Iron-to-Platinum Silyl Ligand Migration: a Combined Experimental and Theoretical Study

Walter Schuh,[†] Pierre Braunstein,*[,†] Marc Bénard,*[,‡] Marie-Madeleine Rohmer,[‡] and Richard Welter[§]

Contribution from the Laboratoire de Chimie de Coordination, UMR 7513 CNRS, Université Louis Pasteur, the Laboratoire de Chimie Quantique, UMR 7551 CNRS, Université Louis Pasteur, and the Laboratoire DECMET, UMR 7513 CNRS, Université Louis Pasteur, 4 rue Blaise Pascal, F-67070 Strasbourg Cédex, France

Received March 4, 2005; E-mail: braunst@chimie.u-strasbg.fr

Abstract: The heterotrinuclear chain complex $Hg[Fe\{Si(OMe)_3\}(CO)_3(dppm\text{-}P)]_2$ (dppm = $Ph_2PCH_2PPh_2$) **1** which has a transoid arrangement of the phosphine donors was used as a versatile chelating metallodiphosphine ligand owing to the easy rotation of its metal core about the Fe−Hg σ-bonds. Its reaction with the labile Pt(0) olefin complex $[Pt(C_7H_{10})_3]$ yielded $[HgPt\{Si(OMe)_3\}Fe_2(CO)_6\{Si(OMe)_3\}(\mu\text{-dppm})_2]$ **5** which resulted, after coordination of the dangling phosphine donors to Pt, from an unprecedented intramolecular rearrangement involving a very rare example of silyl ligand migration between two different metal centers, and the first one in metal cluster chemistry. The major structural differences observed between the heterometallic complexes obtained from **1** and d^{10} Cu(I), Pd(0), or Pt(0) precursors have been established by X-ray diffraction. The bonding situation in the silyl migrated Pt complex **5** was analyzed and compared to those in the isoelectronic, but structurally distinct complexes obtained from Cu(I) and Pd(0) precursors, $[Hg\{Fe[Si(OMe)_3](CO)_3(\mu\text{-dppm})\}_2Cu]^+$ (**2**) and $[Hg\{Fe[Si(OMe)_3](CO)_3(\mu\text{-dppm})\}_2Pd]$ (**4**), respectively, by means of extended Hückel interaction diagrams. DFT calculations then allowed the energy minima associated with the three structures to be compared for **2**, **4**, and **5**. All three minima are in close competition for the Pd complex **4**, but silyl migration is favored by ~10 kcal mol^{-1} for **5**, mainly due to the more electronegative character of Pt with respect to Pd.

Introduction

The selective, directed assembling of complex heterometallic structures is a challenging area of synthetic chemistry that has numerous implications in structural chemistry, chemical bonding, molecular magnetism, reactivity, and catalysis as well as in bioinorganic chemistry.[1] Fine-tuning of the direct or through bridge metal−metal interactions allows unprecedented bonding modes and reactivity patterns for ubiquitous ligands in organometallic chemistry such as alkyl, silyl, and phosphine ligands and is essential for the occurrence of major phenomena such as cooperativity and synergism.[2]

Making use of weak interatomic forces, such as H-bonding or van der Waals interactions, for assembling molecules is central to the development of supramolecular chemistry.[3] Their intramolecular versions have also been known for a long time, but we recently found that relatively weak metal−metal interactions between *chemically different* close-shell metal ions with a d^{10} configuration can also be used to control the conformation of heterometallic mesocycles, i.e., seven- to ten-membered inorganic rings.[4] Relatively few of them contain two or more consecutive transition metals (directly bonded to each other), and heterometallic examples are even rarer.[5] Their often intrinsic flexibility can account for original dynamic behavior, and their molecular conformation and topology should depend not only on the elements that constitute the organic backbone but also on the nature of the metal−ligand interactions. Furthermore, unique properties may result from interactions occurring in directions different from those of the valence orbitals, as shown in the chemistry of gold with "tangential" metal−metal bonding.[6] Although gold is the element of choice for the observation of most pronounced relativistic effects,[7]

[†] Laboratoire de Chimie de Coordination.
[‡] Laboratoire de Chimie Quantique.
[§] Laboratoire DECMET.

(1) (a) *The Chemistry of Metal Cluster Complexes*; Shriver, D. F.; Kaesz, H. D.; Adams, R. D. Eds.; VCH New York, 1990. (b) *Catalysis by Di- and Polynuclear Metal Cluster Complexes*; Adams, R. D., Cotton, F. A., Eds.; Wiley-VCH: New York, 1998. (c) *Metal Clusters in Chemistry*; Braunstein, P., Oro, L. A., Raithby, P. R., Eds.; Wiley-VCH: Weinheim, 1999.
(2) Braunstein, P.; Boag, N. M. *Angew. Chem., Int. Ed.*. **2001**, *40*, 2427.
(3) Lehn, J.-M. *Supramolecular Chemistry. Concepts and Perspectives*; VCH: Weinheim, 1995.
(4) Bénard, M.; Bodensieck, U.; Braunstein, P.; Knorr, M.; Strampfer, M.; Strohmann, C. *Angew. Chem., Int. Ed. Engl.* **1997**, *36*, 2758.
(5) *Comprehensive Organometallic Chemistry*; Abel, E. W., Stone, F. G. A., Wilkinson, G., Eds.; Pergamon: Oxford, U.K., 1995; Vol. 10.
(6) (a) Schmidbaur, H. *Gold Bull*. **1990**, *23*, 11. (b) Mingos, D. M. P. *J. Chem. Soc., Dalton Trans*. **1996**, 561. (c) *Gold: Progress in Chemistry, Biochemistry and Technology*; Schmidbaur, H., Ed.; Wiley: New York, 1999. (d) Schmidbaur, H. *Nature* **2001**, *413*, 31.

10.1021/ja051389z CCC: $30.25

Scheme 1

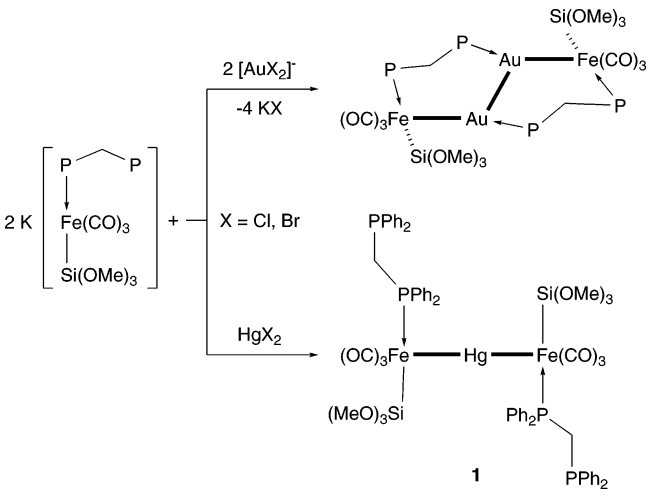

close-shell d^{10} ions other than Au(I), such as Hg(II), are also expected to display interesting structural features. It becomes therefore particularly important to investigate the synthesis, structure, and bonding of closely related molecules in which only the nature of the d^{10} ion could be varied, while keeping the other variables constant. We have previously reported on the competing metal−metal bonding in heterometallic complexes of gold and mercury and contrasted the behavior of the isoelectronic complexes $[AuX_2]^-$ and HgX_2 toward the dppm-substituted silyliron metalate $[Fe\{Si(OMe)_3\}(CO)_3(dppm\text{-}P)]^-$ (dppm = $Ph_2PCH_2PPh_2$).[8] The former d^{10} complex led to an unprecedented Fe−Au−Au−Fe chain complex, whose mercury analogue did not form owing to insufficient d^{10}−d^{10} attractive interaction (Scheme 1).

The heterotrimetallodiphosphine **1**[8] was subsequently shown to act as an excellent ligand for lightly stabilized metal centers with a d^{10}-electron configuration.[4,9,10] Its linear trimetal chain offers both rigidity toward bending, since the preferred coordination geometry about Hg(II) is linear, and adaptability, since free rotation about the metal−metal σ-bonds is easy. The mutually *anti*-type arrangement of the phosphine donors in **1** can thus easily become of the *syn*-type in complexes where it then behaves as a *trans*-spanning, chelating diphosphine.[4,9] This allowed the "capture" of a Cu(I) ion in complex **2**,[4] which is in close-enough proximity to the central mercury to generate an unprecedented transannular bonding interaction, with a Cu−Hg distance determined by X-ray diffraction of only 2.689(2) Å.[4] The corresponding d^{10}−d^{10} interaction, although weak, was found by theoretical calculations to be stabilizing, in agreement with the experimental observations. In view of the current fundamental interest in metallophilic interactions based on relativistic effects and their structural implications,[7] we envisaged using heavier metals that should favor this phenomenon and take advantage of a synthetic approach which allows us to vary only one parameter at a time, namely the nature of the d^{10} center.

Reaction of **1** with Hg^{2+} afforded a Z-shaped complex **3** in which Hg···Hg bonding is likely to occur,[10] whereas with Pd(0) we observed a bonding situation related to that of the Cu(I) complex **1**, except that the Pd−Hg bond in **4** was not perpendicular to the Fe−Hg−Fe axis but the Fe−Hg−Pd angle was only 65.8(6)°.[9] This was explained by the additional

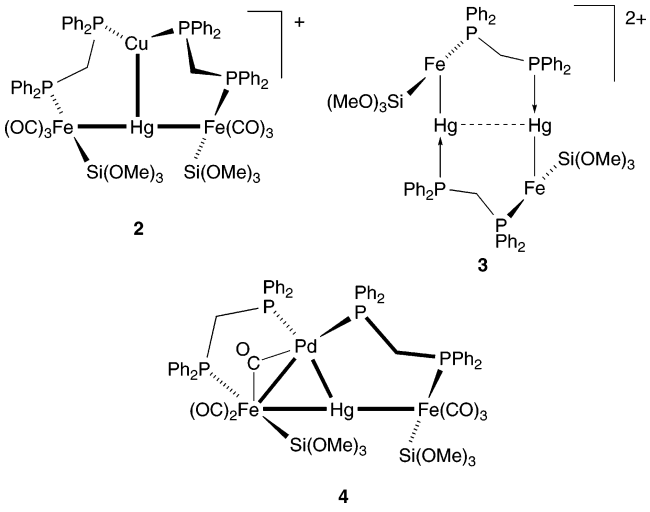

stabilization provided by a semibridging carbonyl ligand belonging to an iron moiety. Variable-temperature NMR studies indicated that the dynamic behavior of **4** involves a sort of oscillation of the Pd atom along the metal chain,[9] whereas the dynamic behavior of **2** was described as that of a molecular torsion pendulum.[4] We have now studied the situation with Pt(0) in place of Pd(0) and found a completely different outcome of its "capture" reaction by **1**. An unprecedented intramolecular rearrangement is observed which includes a very rare example of silyl ligand migration between two different metal centers and the first in metal cluster chemistry. Here we also describe the crystal structure of the new Fe_2HgPt complex and a theoretical analysis of the bonding situations encountered in the three related systems displaying heterometallic d^{10}−d^{10} interactions which result from the reaction of Cu(I), Pd(0), and Pt(0) centers with the chain complex **1**. This set of isoelectronic systems provides a unique opportunity for studying structure/bonding/reactivity relationships both experimentally and theoretically.

Results and Discussion

1. Synthesis and Structures. Following the reactions between **1** and the d^{10} metal complexes $[Cu(NCMe)_4]^+$ and $[Pd_2(dba)_3]$ which afforded the T-shaped complex **2**[4] and **4**,[9] respectively, we investigated the reaction with the Pt(0) complex $[Pt(C_7H_{10})_3]$ in THF (eq 1).

Although ^{31}P NMR monitoring of the reaction mixture (see below) indicated that two chemically different phosphorus atoms were bonded to platinum, it became obvious that the reaction had not proceeded similarly to the Pd case. An X-ray crystal structure determination of **5**·C_6H_6 (Figure 1 and Table 1) confirmed the coordination of both dangling phosphorus atoms of **1** to the Pt center, but although one silyl ligand has remained attached to an Fe center, trans to P(3) as in **1**, the other has unexpectedly migrated from Fe(1) to Pt. The Pt atom adopts an asymmetric, bridging position across one Fe−Hg bond of the Fe−Hg−Fe chain; the resulting spiked-triangular tetranuclear Fe_2HgPt core is somewhat distorted away from planarity. The

(7) Pyykkö, P. *Angew. Chem., Int. Ed.* **2004**, *43*, 4412. Pyykkö, P. *Chem. Rev.* **1997**, *97*, 597 and references cited.
(8) Braunstein, P.; Knorr, M.; Tiripicchio, A.; Tiripicchio Camellini, M. *Inorg. Chem.* **1992**, *31*, 3685.
(9) Schuh, W.; Braunstein, P.; Bénard, M.; Rohmer, M.-M.; Welter, R. *Angew. Chem., Int. Ed.* **2003**, *42*, 2161.
(10) Schuh, W.; Braunstein, P.; Welter, R. *C. R. Chim.* **2003**, *6*, 59.

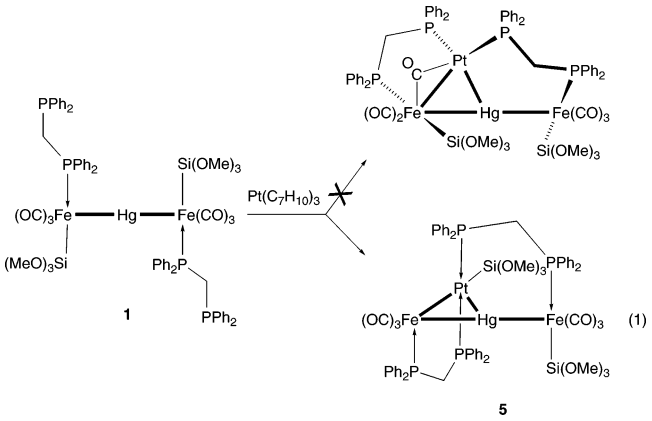

metal core contains an Fe(1)−Hg−Pt triangle which appears to be the first of its kind, while an Fe−Hg−Pt open chain complex is known.[11] The metal−metal distances of 2.569(1) (Fe(1)−Hg), 2.824(1) (Pt−Hg), and 2.955(1) (Pt−Fe(1)) Å all correspond to bonding interactions within the metal triangle, which is metalloligated to a second Fe center by a Hg−Fe(2) bond of 2.570(1) Å. A striking feature is that both Fe−Hg bonds exhibit almost the same length. This is in contrast to **4**, where a 3c−2e interaction between a 14 VE Pd^0 fragment and an Fe−Hg single bond leads to an elongation of the Pd-bridged Fe−Hg bond. The Fe−Hg bonds in the related compounds **2** and **4** range from 2.574(1) to 2.6680(9) Å, the Fe(1)−Pt distance in **5** is considerably longer than those usually found for iron−platinum single bonds (2.63−2.72 Å),[12] and the Hg−Pt separation is in the higher range of the values found for Hg−Pt bonds (2.51−2.83 Å).[11,13] A localized electron count about each metal center in **5** leads to 18, 16, and 14 for Fe, Pt, and Hg, respectively. A possible description of the bonding in the triangular Fe(1)−Hg−Pt fragment corresponds to the view that four valence electrons are responsible for bonding; one of the bonding orbitals is centered between Fe(1) and Hg, whereas the second is delocalized over all three metal atoms. The bonding in the metal triangle is furthermore strengthened by a Pt−Hg d^8−d^{10} interaction. The unusual bonding situation in **5** will be examined below on the basis of theoretical calculations.

The Fe−Hg−Fe chain is significantly bent in **5** with an angle of 164.50(2)°, and the coordination geometry about Fe(2) may be described as distorted octahedral with the P and Si atoms trans to each other and the CO ligands in a *mer* arrangement. The Fe(1) coordination sphere is best described as trigonal bipyramidal, if one counts the Pt−Hg bond as a single "ligand": the P(1), C(1), and C(3) atoms of the coordinated phosphine and carbonyl substituents lie perfectly in an equatorial plane containing Fe1 (Σ P(1)−Fe(1)−C(3), C(3)−Fe(1)−C(1), C(1)−Fe(1)−P(1) = 360°), the third carbonyl, and the Pt−Hg bond, serving as axial ligands. The coordination environment of the platinum center is constituted by two trans phosphine moieties P(2) and P(4) and the silyl group Si(1) which form a T-shaped geometry around Pt (mean P−Pt−Si value 89.6(6)°; P(2)−Pt−P(4) 174.60(4)°), whereas the position trans with respect to the $Si(OMe)_3$ ligand is occupied by the Hg−Fe(1) bond (Si(1)−Pt−Hg 147.27(4)°, Si(1)−Pt−Fe(1) 159.48(3)°).

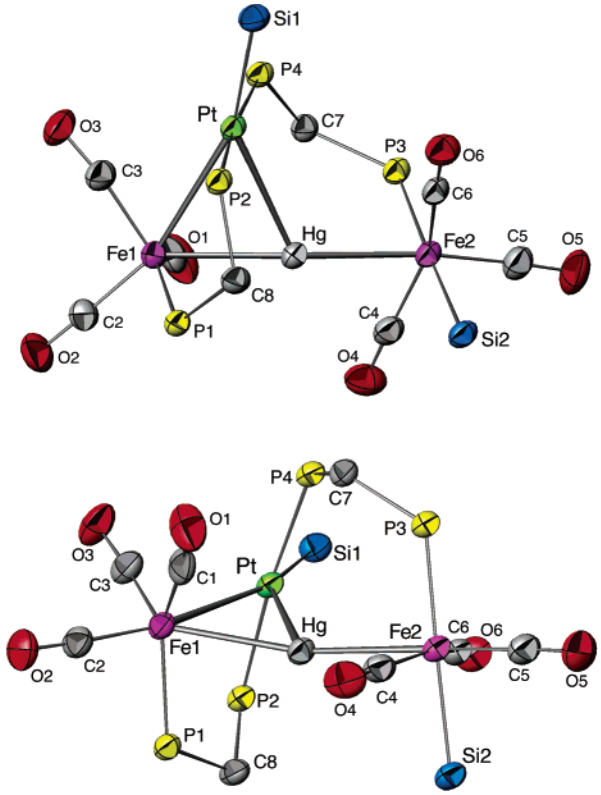

Figure 1. ORTEP views of the molecular structure of **5** in **5**·C_6H_6. The P-phenyl and Si-methoxy groups as well as the solvent molecule have been omitted for clarity. The different perspectives allow a better appreciation for the coordination geometry about the metal centers and the helical arrangement of the Fe(1)P(1)C(8)P(2)PtP(4)C(7)P(3)Fe(2)Si(2) atoms. Thermal ellipsoids enclose 50% of the electronic density.

The Hg−Fe(1) bond is coordinated "upright" to platinum with the Hg−Fe vector quasi-perpendicular to the Pt coordination plane as shown by the dihedral angles given in Table 1. This is reminiscent of the common alkene coordination mode in Pt(II) complexes.[14]

Whereas a dppm ligand bridges the Fe(1)−Pt bond to form a five-membered ring, the other connects the Pt and Fe(2) centers to form a much rarer example of a six-membered ring containing three consecutive and different metal atoms, with a boat-type conformation.[8,11] Noteworthy is the helical arrangement formed by the sequence of atoms Fe(1)P(1)C(8)P(2)PtP(4)-C(7)P(3)Fe(2)Si(2). Since the silyl ligand is best viewed as a

(11) Braunstein, P.; Knorr, M.; Strampfer, M.; Tiripicchio, A.; Ugozzoli, F. *Organometallics* **1994**, *13*, 3038.
(12) (a) Braunstein, P.; Knorr, M.; Hirle, B.; Reinhard, G.; Schubert, U. *Angew. Chem., Int. Ed.* **1992**, *31*, 1583. (b) Braunstein, P.; Knorr, M.; Reinhard, G.; Schubert, U.; Stährfeldt, T. *Chem.—Eur. J.* **2000**, *6*, 4265.
(13) (a) Bennett, M. A.; Contel, M.; Hockless, D. C. R.; Welling, L. L.; Willis, A. C. *Inorg. Chem.* **2002**, *41*, 844−855. (b) Janzen, M C.; Jennings, M. C.; Puddephatt, R. J. *Inorg. Chem.* **2001**, *40*, 1728. (c) Schuh, W.; Kopacka, H.; Wurst, K.; Peringer, P. *Eur. J. Inorg. Chem.* **2001**, 2399. (d) Müller, J.; Zangrando, E.; Pahlke, N.; Freisinger, E.; Randaccio, L.; Lippert, B. *Chem.—Eur. J.* **1998**, *4*, 397. (e) Falvello, R. L.; Fornies, J.; Martin, A.; Navarro, R.; Sicilia, V.; Villarroya, P. *Inorg. Chem.* **1997**, *36*, 6166. (f) Hao, L.; Vittal, J.; Puddephatt, R. J. *Organometallics* **1996**, *15*, 3115. (g) Dahmen, K.-H.; Imhof, D.; Venanzi, L. M.; Gerfin, T.; Gramlich, V. J. *Organomet. Chem.* **1995**, *486*, 37. (h) Krumm, M.; Zangrando, E.; Randaccio, L.; Menzer, S.; Danzmann, A.; Holthenrich, D.; Lippert, B. *Inorg. Chem.* **1993**, *32*, 2183. (i) Albinati, A.; Dahmen, K.-H.; Demartin, F.; Forward, J. M.; Longley, C. J.; Mingos, D. M. P.; Venanzi, L. M. *Inorg. Chem.* **1992**, *31*, 2223. (j) Handler, A.; Peringer, P.; Müller, E. P. *J. Organomet. Chem.* **1990**, *389*, C23. (k) Ghilardi, C. A.; Midollini, S.; Moneti, S.; Orlandini, A.; Scapacci, G.; Dakternieks, D. *J. Chem. Soc., Chem. Commun.* **1989**, 1686. (l) Grishin, Y. K.; Roznyatovskii, V. A.; Ustynyuk, Y. A.; Titova, S. N.; Domrachev, G. A.; Razuvaev, G. A. *Polyhedron* **1983**, *2*, 895.
(14) (a) Hartley, F. R. In *Comprehensive Organometallic Chemistry*; Abel, E. W., Stone, F. G. A., Wilkinson, G., Eds. Pergamon: Oxford, U.K., 1982; Vol. 6, Chapter 39. (b) Young, G. B. In *Comprehensive Organometallic Chemistry*; Abel, E. W., Stone, F. G. A., Wilkinson, G., Eds.; Pergamon: Oxford, U.K., 1995; Vol. 9, Chapter 9.

Table 1. Selected Distances (Å) and Angles (deg) in **5**·C_6H_6

Pt−Hg	2.824(1)
Pt−Fe1	2.955(1)
Hg−Fe1	2.569(1)
Hg−Fe2	2.570(1)
Pt−Si1	2.329(1)
Pt−P2	2.311(1)
Pt−P4	2.339(1)
Hg−P1	3.081(2)
Fe1−P1	2.233(2)
Fe2−P3	2.239(2)
Fe1−Hg−Fe2	164.50(2)
Fe2−Hg−Pt	118.69(3)
Hg−Pt−Fe1	52.72(4)
Fe1−Hg−Pt	66.25(2)
Hg−Fe1−Pt	61.02(3)
Si1−Pt−Hg	147.27(4)
Si1−Pt−Fe1	159.48(3)
P2−Pt−P4	174.60(4)
P2−Pt−Si1	87.56(6)
Si1−Pt−P4	91.73(6)
C2−Fe1−Pt	161.8(2)
C2−Fe1−Hg	137.0(2)
P1−Fe1−Hg	79.47(6)
C1−Fe1−P1	138.5(2)
C1−Fe1−C3	106.3(2)
C3−Fe1−P1	115.3(2)
Fe1−Hg−Pt−P2	83.34(6)
Fe1−Hg−Pt−P4	−101.55(6)
P2−Pt−Fe1−Hg	−96.18(6)
P4−Pt−Fe1−Hg	78.98(6)
Fe1−Hg−Pt−Si1	173.03(6)
Si1−Pt−Fe1−Hg	−169.21(9)

uninegatively charged ligand in complex **1** (with formally d^8 Fe(0) and d^{10} Hg(II) centers), this unexpected ligand migration reaction may be considered as an intramolecular redox process resulting in an electronic situation that can be formally described as: d^8 Fe1(0), d^9 Pt(I), $d^{10}s^2$ Hg(0), and d^7 Fe2(I) or d^8 Fe1(0), d^8 Pt(II), $d^{10}s^2$ Hg(0), and d^8 Fe2(0). This reaction represents a still very rare example of a silyl migration reaction between two metal centers. In homometallic complexes, silyl migration has been observed in diruthenium systems,[15] and the only precedents in heterometallic chemistry concern, to the best of our knowledge, (*i*) phosphido-bridged Fe−Pt complexes where it was triggered by external nucleophiles (CO or isonitriles) and shown to follow an intramolecular, concerted, dyotropic-type mechanism (a type of $[1,2]^2$-migration)[16] and (*ii*) a dppm-bridged Fe−Pt complex[17] and a Pt/Rh complex in which the silyl ligand migrated from Pt to Rh.[18] Quite remarkably, silyl migration involving the Fe/Pt couple was always observed to occur from iron to platinum. Although a thermodynamic balance is difficult to establish in view of the number of bonds broken/created, one of the components that drives the former reaction is the formation of a Pt−Si bond, usually stronger than the Fe−Si bond.[19] In the present case, silyl migration appears to be a characteristic, intrinsic feature of the initial system (**1** + $Pt(C_7H_{10})_3$), and it does not require addition of external reagents.

Multinuclear solution NMR spectroscopic data for **5** are consistent with the structure found in the solid state. The ^1H and ^{31}P NMR studies confirm the dissymmetric structure of the complex; the Pt-bound phosphorus atoms display a 410 Hz ^2J(PP) coupling indicative for their trans arrangement. The ^{29}-Si NMR spectrum exhibits two resonances, one of which shows a pair of ^{195}Pt satellites and proves the migration of the Si-$(OMe)_3$ group from Fe(1) to Pt. The ^{195}Pt resonance is in the expected range,[20] whereas the ^{199}Hg resonance is markedly deshielded.[21] The ^{1+2}J(Hg−Pt) coupling constant of 2300 Hz is small compared to the usual ^1J(Hg−Pt) values which range from 37 610 to 2783 Hz.[13]

The $^{31}P\{^1H\}$ NMR spectra of a freshly prepared sample of **5** always showed weak signals due to a second species (about 5−10% of the intensity of the signals of **5**). The appearance of two symmetric quartets (intensities ca. 1:1:1:1) was interpreted as an $[AX]_2$ pattern (δ 54.0, 30.4 ppm in C_6D_6, $N = 72$, separation of the inner lines 14 Hz; δ 53.7, 30.0 ppm in CD_2Cl_2, $N = 74$, separation of the inner lines 21 Hz). This could be indicative of a symmetric compound or of an asymmetric compound undergoing a fast enough dynamic exchange on the NMR time scale to make the two respective phosphorus atoms chemically equivalent (eq 2).

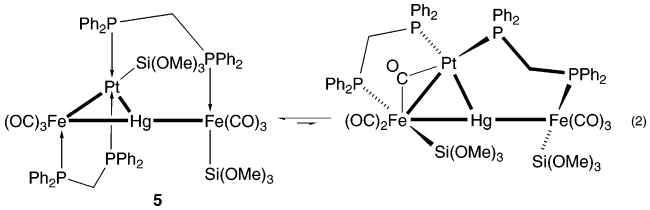

(2)

On the basis of the coupling patterns and the range of chemical shifts, a structure similar to **2** or **4** seems reasonable for this species. To clarify this point and examine whether complex **5** could exist in solution in the form of more than one isomer, comparative theoretical calculations on the bonding and relative stabilities of the different structures found for **2**, **4**, and **5** and their isomers were performed.

2. Quantum Theoretical Models of the Fe_2HgCu, Fe_2HgPd, and Fe_2HgPt Complexes. 2.1. Analysis of the Bonding through EHMO Interaction Diagrams. Figures 2 and 3 display the main interactions occurring between the frontier orbitals of the molecular fragments in complexes **2** and **4**, according to extended Hückel calculations. The average Fe−Hg−Fe axis is assumed collinear to *x*. In both complexes, the metal orbitals of each iron moiety comply with the standard scheme of the square pyramidal coordination, with a low-lying set of t_{2g} orbitals and a d_{x^2}-like orbital higher in energy.[22] The presence of a trimethoxysilyl ligand, traditionally considered anionic, in the coordination sphere of Fe may appear confusing, since silicon is quite electropositive and the weight of the metal

(15) (a) Akita, M.; Oku, T.; Hua, R.; Moro-Oka, Y. *J. Chem. Soc., Chem. Commun.* **1993**, 1670. (b) Akita, M.; Hua, R.; Oku, T.; Tanaka, M.; Moro-Oka, Y. *Organometallics* **1996**, *15*, 4162. (c) Lin, W.; Wilson, S. R.; Girolami, G. S. *J. Am. Chem. Soc.* **1993**, *115*, 3022. (d) Lin, W.; Wilson, S. R.; Girolami, G. S. *Organometallics* **1994**, *13*, 2309. (e) Shelby, Q. D.; Lin, W.; Girolami, G. S. *Organometallics* **1999**, *18*, 1904.
(16) (a) Braunstein, P.; Knorr, M.; Hirle, B.; Reinhard, G.; Schubert, U. *Angew. Chem., Int. Ed.* **1992**, *31*, 1583. (b) Braunstein, P.; Knorr, M.; Reinhard, G.; Schubert, U.; Stährfeldt, T. *Chem.—Eur. J.* **2000**, *6*, 4265.
(17) Braunstein, P.; Faure, T.; Knorr, M. *Organometallics* **1999**, *18*, 1791.
(18) Tanabe, M.; Osakada, K. *Inorg. Chim. Acta* **2003**, *350*, 201.
(19) Aylett, B. J. *Adv. Inorg. Chem. Radiochem.* **1982**, *25*, 1.
(20) Pregosin, P. S. In *Transition Metal Nuclear Magnetic Resonance*; Pregosin, P. S., Ed.; Elsevier: 1991; p 217.
(21) (a) Schuh, W.; Haegele, G.; Olschner, R.; Lintner, A.; Dvortsak, P.; Kopacka, H.; Wurst, K.; Peringer, P. *J. Chem. Soc., Dalton Trans.* **2002**, 19 and references cited therein. (b) Granger, P. In *Transition Metal Nuclear Magnetic Resonance*; Pregosin, P. S., Ed.; Elsevier: 1991; p 306.
(22) Albright, T. A.; Burdett, J. K.; Whangbo, M. H. *Orbital Interactions in Chemistry*; Wiley: New York, 1985; p 312.

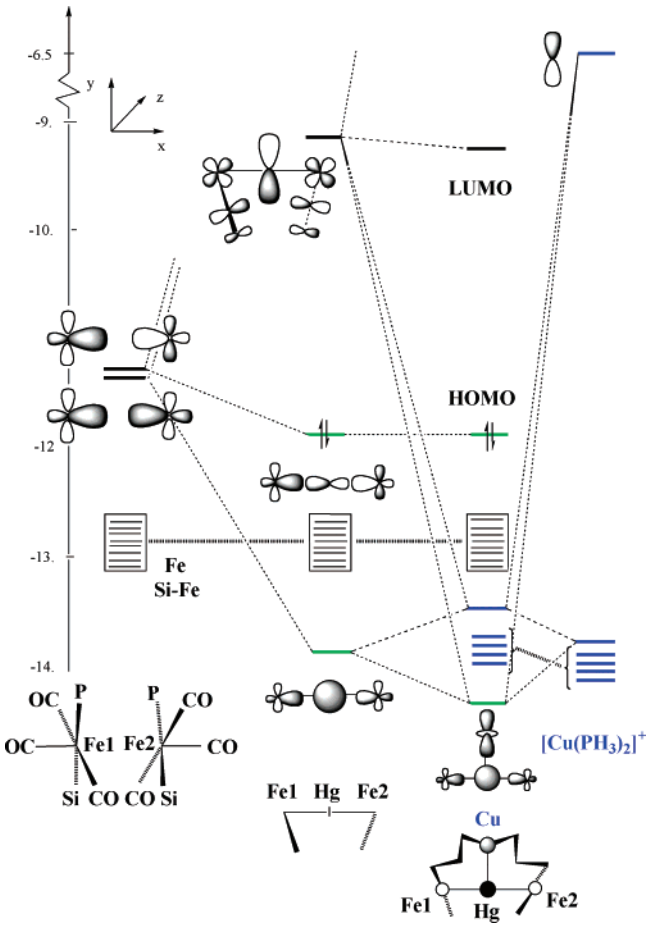

Figure 2. Interaction diagram for a model of complex **2**.

remains dominant in the orbital supposed to describe the $[Si(OMe)_3]^- \rightarrow$ Fe donation.[23] In the fragment dimer, the Fe-silyl orbitals are buried among the Fe t_{2g} orbital combinations. Whereas the silyl fragment is close to electroneutrality, *the charge on silicon itself remains strongly positive*. The bonding of the Fe fragments with mercury, similar in **2** and **4**, can be described in terms of a three-center/four-electron bond: the in-phase combination of the Fe d_{x^2}-like orbitals gives rise to a bonding combination with the low-lying s orbital of Hg, whereas the out-of-phase combination is stabilized through a donation to the p_x orbital of mercury. This latter orbital remains the HOMO in the cationic complex of copper. The LUMO is centered on the p_y orbital of Hg, interacting with iron and donating to the π^* orbitals of the closest carbonyls. The interaction of the low-lying d-shell of Cu^+ with the trinuclear complex splits the in-phase Fe−Hg−Fe orbital, and both resulting MOs receive a stabilizing contribution from the p_y orbitals of Hg and Cu, the latter being obviously much weaker in view of the high energy of the metal p shell in the diphosphine fragment (Figure 2). The bonding between Cu and Hg can be eventually understood in terms of a reciprocal donation from the inner valence shell of one metal to the outermost p_y orbital of the other. Such a dual charge transfer between formally closed-shell metal atoms could be assimilated to the two components of the "ionic" term that was shown to be a second contributor, after dispersion, to the metallophilic attraction between Pd(II) and Au(I).[24]

(23) Zheng, C.; Hoffmann, R. *Inorg. Chem.* **1989**, *28*, 1074.

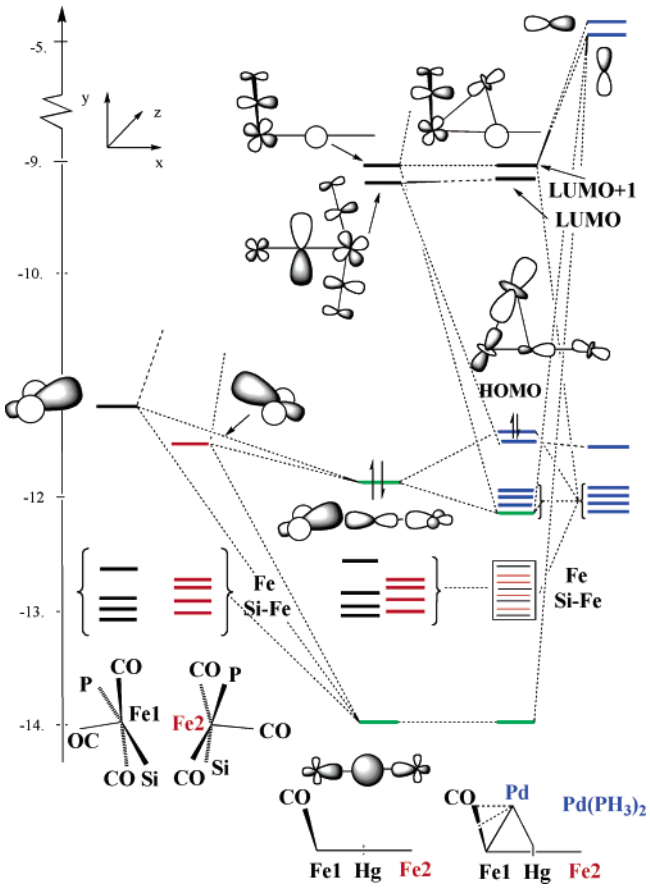

Figure 3. Interaction diagram for a model of complex **4**.

At variance with copper, the d shell of palladium is relatively high in energy. The five occupied orbitals of the $Pd(PR_3)_2$ fragment are now in proper position to split the *HOMO* of the Fe−Hg−Fe fragment (Figure 3). Both terms of the four-electron interaction are stabilized with back-donation interactions, which now primarily affect a carbonyl ligand of Fe1 attached to palladium in a semibridging position. The importance of this interaction is illustrated in the LUMO+1 (Figure 3) which drags into the unoccupied set a relatively large component from the Pd(0) d shell. Donation to the p_y orbital of palladium now originates in orbitals with Fe1−Hg bonding character, represented in green in Figure 3. This donation accounts for the elongation of 0.05 Å observed and computed at the DFT level for the Fe1−Hg bond with respect to Fe2−Hg (Table 3). Back-donation from palladium toward the p shells of Hg and, to some extent, of Fe1 are also expected to significantly contribute to the bonding between the three metal atoms.

The frontier orbitals of the platinum complex **5**, exhibiting the migration of one trimethoxysilyl fragment from Fe1 to Pt, are analyzed in Figures 4 and 5. Figure 4 represents the interactions in the nonsymmetric Fe1−Hg−Fe2 fragment. The migration of the silyl ligand yields a tetracoordinate Fe1 fragment and raises the energy of a hybridized d_{xy} orbital of iron. The three-center/four-electron bond involving Fe1, Fe2, and Hg characterized in complexes **2** and **4** still occurs in **5** (green levels in Figures 4 and 5), but another orbital, very close in energy to the upper term of this delocalized interaction, can

(24) Crespo, O.; Laguna, A.; Fernández, E. J.; López-de-Luzuriaga, J. M.; Jones, P. G.; Teichert, M.; Monge, M.; Pyykkö, P.; Runeberg, N.; Schütz, M.; Werner, H.-J. *Inorg. Chem.* **2000**, *39*, 4786.

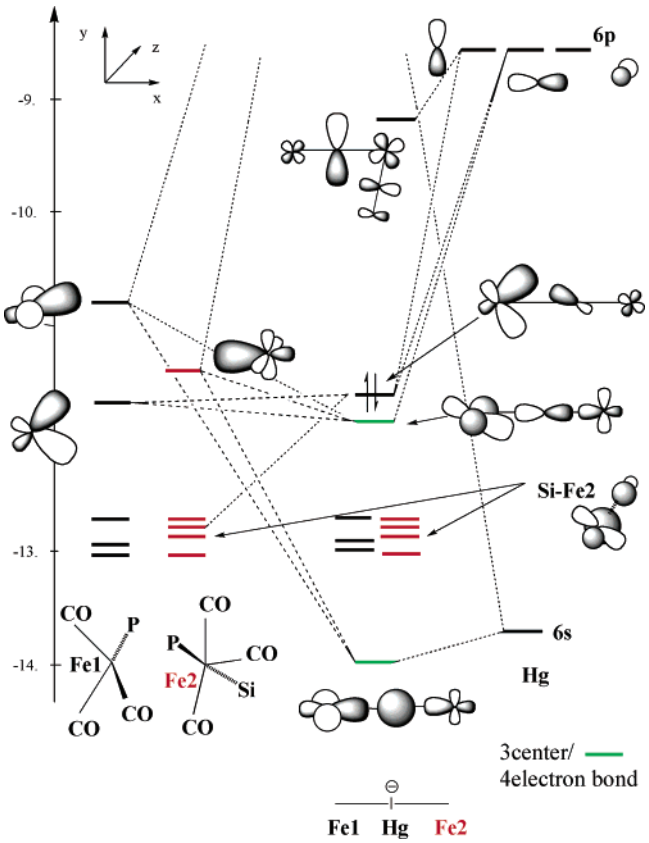

Figure 4. Interaction diagram for the trinuclear Fe−Hg−Fe fragment of **5**.

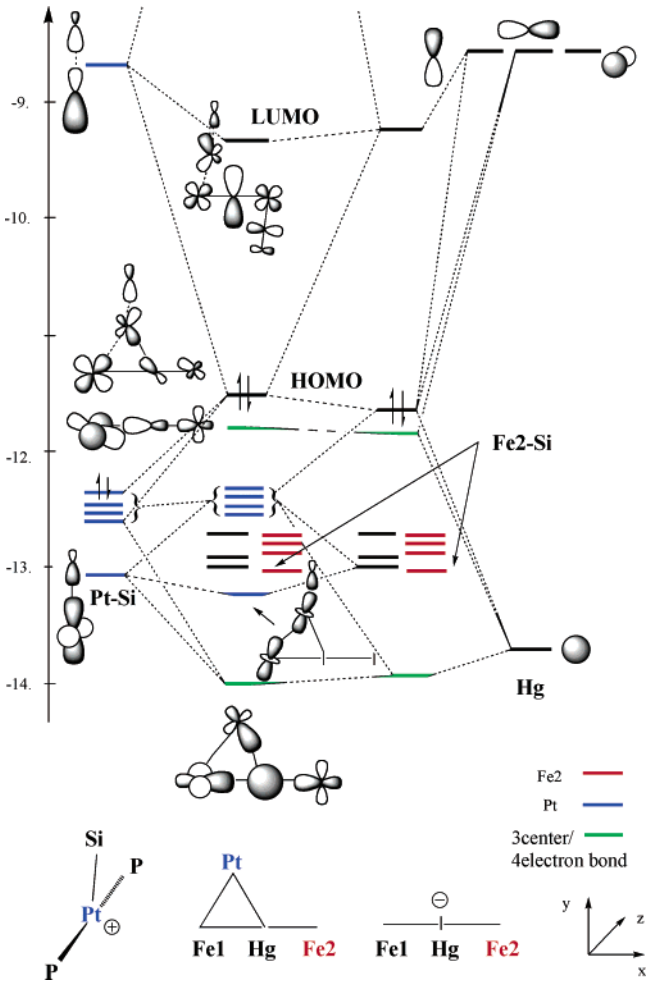

Figure 5. Interaction diagram for complex **5**.

be described in terms of a donation from the d_{xy} orbital of Fe1 to the p shell of Hg (Figure 4). It clearly appears from the sequence of orbital energies that this orbital should be the fragment HOMO. The double occupancy of this level raises the question of the fragment charge, which clearly reflects the ambiguous status of the silyl ligand. The migration of an anionic silyl would result in a cationic Fe−Hg−Fe moiety and in an anionic platinum fragment, both unrealistic with respect to the fragment orbital occupancies. The opposite scheme, retained in Figures 4 and 5, emphasizes the consistency of considering the migrating silyl as an electrophilic moiety.

The orbitals of the $Pt(PR_3)_2Si(OMe)_3$ fragment are displayed in Figure 5, left-hand side. A Pt−Si bonding orbital appears below the block of platinum d orbitals, but, as already noticed by Zheng and Hoffmann, this orbital has its major weight on the platinum d orbital.[23] This orbital is in position to interact with the Fe−Hg−Fe fragment and gives rise to two MOs with bonding character, either with Hg, or with Fe1 (Figure 5). At higher energies, the HOMO of the Fe−Hg−Fe fragment is destabilized due to its interaction with the platinum d block, but the energy raise remains moderate due to a favorable interaction with the p_y orbital of platinum, made readily accessible by the presence of the silyl ligand (Figure 5).

2.2. DFT-Computed Equilibrium Conformations for Models of 2, 4, 5, and Their Relative Energies. DFT calculations have been carried out on models of complexes **2**, **4**, and **5** in which the C_6H_5 and CH_3 substituents in dppm and trimethoxysilyl ligands, respectively, have been replaced by hydrogen atoms. Real $Si(OMe)_3$ groups were considered for some calculations on the palladium complex **4** (Table 2). Calculations show that, for each molecule, all three structural shapes observed

Table 2. Relative Energies (kcal mol^{-1}) Computed for Models of **2**, **4**, and **5** in Each of the Three Observed Conformations: (**A**) C_2 symmetry axis collinear to the M−Hg Bond; (**B**) Bent M−Hg Bond; (**C**) Silyl Migration[a]

conformation	2[b]	4[b]	4[c]	5[b]
A	+0.6 *(0.0)*	+2.2 *(+2.4)*	+1.1	+9.8 *(+9.7)*
B	0.0 *(+0.5)*	0.0 *(0.0)*	0.0	+9.4 *(+9.3)*
C	+32.2 *(+30.9)*	+3.0 *(+3.3)*	+1.5	0.0 *(0.0)*

[a] In roman: relative energies calculated with BP86, from geometries optimized with the same functional. In italics: relative energies calculated with PW91, from the same geometries. [b] Silyl ligand modeled as $Si(OH)_3$. [c] Calculations carried out with the real $Si(OMe)_3$ ligand.

for **2**, **4**, and **5** and referred to as **A**, **B**, and **C**, respectively, correspond to energy minima, either local or global. For each molecule considered, the three minima are all close in energy with a single exception, which excludes the possibility of silyl migrating in the Cu(I) compound (Table 2). The bent conformation **B** that has been crystallographically characterized for the palladium complex **4** was computed to be the global minimum not only for two models of **4** but also for the model of the Cu^+ complex **2**. However, the energy difference with the symmetric (C_2) conformation **A** does not exceed 1.1 kcal mol^{-1} for the most elaborate model of **4** and 0.6 kcal mol^{-1} for **2**. Note that the use of the PW91 functional for single-point calculations on the geometries optimized with BP86 does not appreciably modify the relative energy differences, even though the relative stabilities of conformations **A** and **B** are reversed for **2** (Table

Table 3. Key Geometrical Parameters (Distances in Å, Angles in deg) Obtained for Models of **2**, **4**, and **5** in the Equilibrium Structures Corresponding to Conformations **A** (C_2 Symmetry Axis Collinear to the M−Hg Bond); **B** (Bent M−Hg Bond); and **C** (Silyl Migration)[a]

	2[b]			**4**[b]			**5**[b]		
	A	**B**	**C**	**A**	**B**	**C**	**A**	**B**	**C**
Fe1−Hg	2.66 *(2.61)*	2.80	2.64	2.69	2.74 *(2.67)*	2.63	2.70	2.74	2.64 *(2.57)*
Fe2−Hg	2.66 *(2.61)*	2.63	2.63	2.69	2.68 *(2.62)*	2.69	2.70	2.68	2.69 *(2.57)*
Hg-M	2.77 *(2.69)*	2.68	2.91	2.83	2.79 *(2.69)*	2.94	2.86	2.82	2.94 *(2.82)*
Fe1-M	3.97	2.81	2.74	4.21	2.96 *(2.91)*	2.95	4.25	2.99	2.95 *(2.95)*
M-Si			2.435			2.377			2.366 *(2.33)*
$M-C_{sb}$		2.21			2.12 *(2.14)*			2.11	
$M-O_{sb}$		2.77			2.81 (*2.80*)			2.85	
C_{sb}-O_{sb}		1.180			1.192 (*1.20*)			1.196	
Fe1−Hg−Fe2	172.0 *(176.6)*	173.4	161.7	161.7	171.0 *(175.0)*	163.8	160.5	171.5	164.5 *(164)*
Fe1−Hg-M	94.0 *(92.0)*	61.7	58.9	99.2	64.8 (*65.8*)	63.8	99.7	65.0	66.2 *(66)*
Fe2−Hg-M	94.0 *(92.0)*	119.8	107.7	99.2	122.1 (*118.4*)	110.5	99.7	121.0	111.4 *(119)*

[a] Observed geometrical parameters are given in italics. [b] Silyl ligand modeled as $Si(OH)_3$.

Table 4. Hirshfeld Charges (e) Computed for Models of **2**, **4**, and **5** in the **A**, **B**, and **C** Conformations

	2 (M = Cu)			**4** (M = Pd)			**5** (M = Pt)		
	A	**B**	**C**	**A**	**B**	**C**	**A**	**B**	**C**
M	+0.17	+0.16	+0.19	+0.06	+0.20	+0.25	−0.14	+0.02	+0.05
Hg	+0.34	+0.34	+0.33	+0.30	+0.31	+0.29	+0.32	+0.33	+0.31
Fe1	−0.16	−0.16	−0.16	−0.16	−0.18	−0.19	−0.16	−0.17	−0.17
Fe2	−0.16	−0.16	−0.16	−0.16	−0.16	−0.17	−0.16	−0.16	−0.17
Si1[a]	+0.39	+0.39	+0.39	+0.38	+0.37	+0.30	+0.38	+0.37	+0.33
Si2[b]	+0.39	+0.39	+0.38	+0.38	+0.38	+0.37	+0.38	+0.38	+0.37

[a] Silicium attached to Fe1 (forms **A** and **B**) or to M (form **C**). [b] Silicium attached to Fe2.

2). Anyhow, these energy differences are at the limit of significance of both the computational and the chemical models, since the replacement of $Si(OH)_3$ by $Si(OMe)_3$ in **4** induces differences of 1.1 and 1.5 kcal mol^{-1} in the relative energies (Table 2). The migration of a silyl group resulting in conformation **C** appears quite preferable for **5**, with an advantage of ∼10 kcal mol^{-1} with respect to the other isomers. Note however that form **C** is also competitive for the palladium complex **4**, with a computed energy difference of 1.5 kcal mol^{-1} only with respect to the observed conformation, according to the most elaborate model. Even though no evidence has been obtained from experiment, two or even three conformations of the palladium complex could possibly coexist in solution.

Energy differences are larger for the platinum compound. The stabilization by ∼10 kcal mol^{-1} of the silyl migrated isomer cannot be assigned to a specific weakness of the Pt−Hg or Pt−CO interactions in forms **A** and **B**, respectively, since no significant changes concerning key geometrical parameters were calculated with respect to the Pd complex (Table 3). The silyl migrated (**C**) isomers of complexes **4** and **5** are also structurally similar, except for a tiny contraction (0.01 Å) of the Si−M distance with platinum. This suggests that the relative stabilities of the **B** and **C** isomers are governed rather by electrostatic factors than by a change in the interaction between frontier orbitals. Indeed, the more electronegative character of Pt with respect to Pd makes the metal more attractive to silicon, as evidenced by the Hirshfeld charge analysis (Table 4). The atomic charges of the Fe−Hg−Fe framework are remarkably stable whatever may be the d^{10} metal M and the molecular conformation. The charge on silicon is always largely positive, close to +0.4e when the silyl ligand is coordinated to Fe, and to +0.3e for the migrated Si in conformation **C** (M = Pd, Pt). However, the charge on M varies with both the molecular structure and the nature of M (Table 4). The charge of Pd and Pt decreases by ∼0.15e from the symmetric form **A** to the bent form **B**, due to the back-donation toward the semibridging CO. The charge is still lower, i.e., positive, in form **C**, but the relative depopulation of Pd with respect to Pt (∼0.2e) definitely provides the latter an electrostatic advantage in its interaction with the silyl ligand.

Table 3 displays selected geometrical parameters computed for the three conformations of **2**, **4**, and **5**. The bond lengths and angular parameters computed for the structure observed in the crystal are in good agreement with the values obtained from X-ray diffraction, given the systematic tendency of GGA functionals to overestimate interatomic distances in coordination compounds. The comparison between the equilibrium distances computed for the three isomers of each complex confirms some trends deduced from orbital analysis. It first appears that the low-lying d shell of copper is less prone than Pd or Pt to back-donate electron density to a semi-bridging CO. In conformation **B** of complex **2**, the $Cu-C_{sb}$ distance is longer than that in **4B** and **5B** by ∼0.1 Å and the activation of the CO bond is less pronounced. This weak back-donation is compensated by an important charge transfer from the Fe1−Hg bond to the relatively low-lying $5p_{x,y}$ orbitals of the copper diphosphine moiety. This results in a conspicuous stretching (0.14 Å) of the Fe1−Hg bond with respect to isomer **A**, combined with short Cu−Hg and Cu−Fe1 bonds (Table 3) and makes isomer **B** energetically competitive with the observed form **A** (Table 2). It is also clear that form **C** is penalized due to a poor coordination of the silyl fragment to copper, resulting in a Cu−Si distance longer than Pd−Si and Pt−Si in the same bonding mode.

It can also be noted that the shift from isomer **A** to **B** or **C** in the Pd/Pt complexes yields opposite responses of the Fe1−Hg bond, whereas the Fe2−Hg distance remains stable at ∼2.69 Å (Table 3). As in the copper system, the Fe1−Hg bond is weakened in form **B** as a consequence of donation toward the outer p shell of Pd/Pt, but at variance with copper, the bond stretching remains moderate (∼0.05 Å). The same bond *contracts* by a similar amount in form **C** (Table 3) due to the polarization of the Fe−Hg−Fe bonding interactions toward Fe1 induced by the silyl migration (Figure 5). The stretching of Fe1−Hg alone (0.06 Å) is observed in the crystal structure of **4**, but X-ray diffraction indicates that *both* Hg−Fe distances in **5** have been reduced by 0.04 Å with respect to the observed, symmetric structure of **2** (Table 3).

Conclusion

The heterotrinuclear chain complex [Hg{Fe[Si(OMe)$_3$](CO)$_3$(dppm-*P*)}$_2$] (dppm = $Ph_2PCH_2PPh_2$) **1** which has a transoid arrangement of the phosphine donors was used as a versatile chelating metallodiphosphine ligand owing to the easy rotation of its metal core about the Fe−Hg σ-bonds. Whereas its reaction with labile Cu(I) or Pd(0) precursor complexes led to chelation of the d^{10} center by the P donors and generation of heterometallic $d^{10}-d^{10}$ interactions with the Hg(II) center, the reaction with the labile Pt(0) complex [Pt(C_7H_{10})$_3$] yielded [HgPt{Si(OMe)$_3$}Fe$_2$(CO)$_6$\{Si(OMe)$_3$\}(μ-dppm)$_2$] **5** which resulted, in addition to coordination of the dangling phosphine donors to Pt, from an unprecedented intramolecular rearrangement involving a very rare example of silyl ligand migration between two different metal centers, and the first one in metal cluster chemistry. The major structural differences observed between the heterometallic complexes formed from the reaction between **1** and Pd(0) or Pt(0) precursors as well as the unusual electronic situation within the heterotrimetallic metal−metal bonded core of **5** were analyzed by means of extended Hückel interaction diagrams. DFT calculations then allow the energy minima associated with the three structures to be compared for **2**, **4**, and **5**. All three minima are in close competition for the Pd complex **4**, but silyl migration is favored by ~10 kcal mol^{-1} for **5**, mainly due to the more electronegative character of Pt with respect to Pd. These results emphasize the consequences that subtle differences within a series of closely related d^{10} systems may have on the nature, bonding, and behavior of complex heterometallic molecules.

Experimental Section

All manipulations were carried out in absolute solvents under standard Schlenk conditions; compounds **1** and Pt(C_7H_{10})$_3$ were prepared according to the literature.[8,25] The ^{1}H{^{31}P}, ^{31}P{^{1}H}, ^{29}Si{^{1}H}, ^{195}Pt{^{1}H}, and ^{199}Hg{^{1}H} NMR spectra were recorded on Bruker AV 400 and AV 300 instruments; chemical shifts are reported in ppm and were referenced to TMS (^{1}H, ^{29}Si), external 85% H_3PO_4 (^{31}P), 1 mol/l Na_2PtCl_6 (^{195}Pt), and neat $HgMe_2$ (^{199}Hg), respectively, and coupling constants are reported in Hertz. The NMR spectra were recorded at 298 K, unless otherwise stated. IR spectra were recorded on a Perkin-Elmer FT-IR 1600 instrument, and FAB-MS spectra, on an autospec HF mass spectrometer.

Complex 5: Compound **1** (343 mg, 0.230 mmol) and [Pt(C_7H_{10})$_3$] (110 mg, 0.230 mmol) were dissolved in THF (20 mL) at −30 °C and left to warm to room temperature under vigorous stirring. The resulting dark yellow solution was evaporated to dryness, and the solid residue was redissolved in THF (20 mL), filtered over Celite, and evaporated to dryness. The resulting solid was recrystallized from C_6H_6/pentane by vapor diffusion at room temperature. Compound **5** crystallized in the form of dark brown blocks as a C_6H_6 solvate. Yield: 170 mg (44%). Anal. Calcd for $C_{62}H_{62}Fe_2HgO_{12}P_4PtSi_2$ (1686.6): C, 44.15; H, 3.71. Found: C, 43.81; H, 3.68%. IR (Nujol): ν (cm^{-1}) = 1990 (m), 1945 (sh), 1903 (vs), 1884 (s), 1845 (s). ^{1}H{^{31}P} NMR (C_6D_6, 283 K): δ = 8.90−6.40 (m, 40 H, Ph), 4.98 (d, 1 H, ^2J(H−C−H) = 13.8, CH_2), 4.78 (d, 1 H, ^2J(H−C−H) = 13.8, CH_2), 4.35 (d, 1 H, ^2J(H−C−H) = 13.8, CH_2), 3.69 (d, 1 H, ^2J(H−C−H) = 13.8, CH_2), 3.91 (s, 9H, $(MeO)_3SiFe$), 2.62 (s, 9H, $(MeO)_3SiPt$). From variable temperature ^{1}H{^{31}P} NMR experiments, a dynamic exchange of **5** in solution can be deduced, since the four dppm methylene resonances become broad upon warming. This is tentatively interpreted as the beginning of a torsion motion of the dppm backbones and the Pt atom about the Fe−Hg−Fe axis. Since complex **5** decomposes rapidly in solution at 50 °C before reaching the coalescense temperature, no activation parameters could be determined in order to quantify and better describe the mechanism of the dynamic behavior. ^{31}P{^{1}H} NMR (C_6D_6): δ = 53.8 (d, ^2J(P^4,P^3) = 10 Hz, P^3), 48.1 (dd, ^{3+4}J(P^1,P^4) = 14 Hz, ^{2+3}J(P^1,P^2) = 72 Hz, ^{2+3}J(Pt,P^1) = 12 Hz, ^2J(Hg,P^1) = 545 Hz, P^1), 25.5 (dd, ^2J(P^2,P^4) = 410 Hz, ^1J(Pt,P^2) = 2928 Hz, P^2), 9.8 (ddd, ^1J(Pt,P^4) = 2744 Hz, P^4). ^{29}Si{^{1}H} NMR (C_6D_6): δ = 2.8 (d, ^2J(P,Si) = 25 Hz, Si^2), −50.5 (s, ^1J(Pt,Si) = 1960 Hz, Si^1). ^{195}Pt{^{1}H} NMR (C_6D_6): δ = −4913 (dd, ^1J(Hg,Pt) = 2300 Hz). ^{199}Hg{^{1}H} NMR (C_6D_6): δ = 498 (d). MS (FAB+, 2-NPOE): m/z = 1686.1 (M$^+$), 1655.1 (M$^+$ − OCH_3), 1630.1 (M$^+$ − 2CO), 1565.1 (M$^+$ − Si(OMe)$_3$), 1486.1 (M$^+$ − Hg), 1425.2 (M$^+$ − Fe(CO)$_3${Si(OMe)$_3$}), 1225.2 (M$^+$ − Hg − Fe(CO)$_3${Si(OMe)$_3$}), 1085.3 (M$^+$ − Hg − Fe(CO)$_3$ − Fe(CO)$_3${Si(OMe)$_3$}), 933.1 (M$^+$ − Hg − Fe(CO)$_3$ − dppm − CO), 840.1 (M$^+$ − Hg − Fe(CO)$_3${Si(OMe)$_3$} − dppm), 756.1 (M$^+$ − Hg − Fe(CO)$_3${Si(OMe)$_3$} − Fe(CO) − dppm).

Computational Details. All geometry optimizations have been performed using the formalism of the density functional theory (DFT), with the gradient-corrected Becke-Perdew/86 (BP86) functional.[26] Calculations have been carried out with the 1999 release of the ADF program[27] based upon the use of Slater basis sets.[28] The basis sets used in the present calculations are referred to as IV or TZP in the ADF User's Guide and have been used in conjunction with the zero-order regular approximation (ZORA) to the relativistic effects. For first row atoms, the 1s shell was frozen and described by a double-ζ Slater function. The neon core of Si, P, Fe, and Cu atoms, the Ar core of Pd, as well as the Kr core of Pt and Hg were also modeled by a double-ζ, frozen Slater basis. The valence shell of all atoms, including the (n + 1)s shell of metals and the 4f shell of Pt and Hg are triple-ζ, whereas the (n + 1)p shell of metals is described by a single orbital. These sets were supplemented with one polarization function for all nonmetal atoms. Single-point calculations at the optimized geometries associated with the energy minima were carried out with the PW91 exchange-correlation functional,[29] which is expected to more accurately account for the dispersion forces.[30] The atomic charges displayed in the present work refer to Hirshfeld's definition of a "promolecule" considered as a superposition of noninteracting neutral atoms.[31] The Hirshfeld charge of atom A corresponds to the integration over space of the density changes induced by chemical bonding on the density of *A*:

$$qA = \frac{\int \rho_{\mathrm{mol}} \times \int \rho_{\mathrm{A}}}{\sum_A \int \rho_{\mathrm{A}}} \qquad (1)$$

Contrary to Mulliken charges, Hirshfeld charges are not artificially sensitive to changes in the basis set. Finally, the qualitative analysis of the bonding between metallic fragments was carried out by means of extended Hückel (EHMO) calculations,[32] using atomic parameters available in the Supporting Information.

(25) Crascall, L. E.; Spencer, J. L. *Inorg. Synth.* **1990**, *28*, 126.

(26) (a) Becke, A. D. *Phys. Rev.* **1988**, *A38*, 3098. (b) Perdew, J. P. *Phys. Rev.* **1986**, *B33*, 8882; **1986**, *B34*, 7406.

(27) (a) *User's Guide, Release 1999;* Chemistry Department, Vrije Universiteit: Amsterdam, The Netherlands, 1999. (b) Baerends, E. J.; Ellis, D. E.; Ros, P. *Chem. Phys.* **1973**, *2*, 41. (c) te Velde, G.; Baerends, E. J. *J. Comput. Phys.* **1992**, *99*, 84. (d) Fonseca-Guerra, C.; Visser, O.; Snijders, J. G.; te Velde, G.; Baerends, E. J. *Methods and Techniques in Computational Chemistry: METECC-95*; Clementi, E., Corongiu, G., Eds.; STEF: Cagliari, Italy, 1995; pp 305−395.

(28) (a) Snijders, J. G.; Baerends, E. J.; Vernooijs, P. *At. Nucl. Tables* **1982**, *26*, 483. (b) Vernooijs, P.; Snijders, J. G.; Baerends, E. J. *Slater type basis functions for the whole periodic system;* Internal Report, Free University of Amsterdam: Amsterdam, The Netherlands, 1981.

(29) Perdew, J. P.; Wang, Y. *Electronic Structure of Solids, 1991*; Ziesche, P., Eschrig, H., Eds.; Akad. Verlag Berlin: Berlin, 1991.

(30) (a) Wesolowski, T. A.; Parisel, O.; Ellinger, Y.; Weber, J. *J. Phys. Chem.* **1997**, *101*, 7818. (b) Lorenzo, S.; Lewis, G. R.; Dance, I. *New J. Chem.* **2000**, *24*, 295.

(31) Hirshfeld, F.; Rzotkiewicz, S. *Mol. Phys.* **1974**, *27*, 1319.

(32) (a) Hoffmann, R.; Lipscomb, W. N. *J. Chem. Phys.* **1962**, *36*, 2179; *37*, 2872. (b) Hoffmann, R. *J. Chem. Phys.* **1963**, *39*, 1397.

X-ray Structure Determination for 5·C_6H_6. Triclinic, space group $P\bar{1}$, $a = 12.9160(2)$ Å, $b = 13.0270(2)$ Å, $c = 21.0590(2)$ Å; $\alpha = 101.032(2)°$, $\beta = 100.739(2)°$, $\gamma = 91.618(2)°$; $V = 3409.42(8)$ Å^3, $Z = 2$, $T = 173(2)$ K, Mo Kα ($\lambda = 0.709\ 30$ Å), 19 762 data collected, 15 055 data with $I > 2\sigma(I)$, θ min/max = 2.41/30.02°. The structure was solved by direct methods (SHELXS-97) and refined by full-matrix least-squares methods on F^2 (SHELXL-97).[33] $R = 0.0360$, $wR2$(all data) = 0.0956, GOF = 1.016. All non-hydrogen atoms of the complex were refined anisotropically, and hydrogen atoms were placed at calculated ideal positions. A cocrystallized benzene molecule was found disordered over two positions (C70−C75, C76−C81) with occupancies of 0.5. The C-atoms of the solvent molecule were refined isotropically, C−C bond lengths were fixed to 1.39 Å, and the respective two C_6 arrangements were restricted to be planar. Hydrogen atoms at C_6H_6 were not included in the calculations.

Acknowledgment. Dedicated to Prof. H. W. Roesky on the occasion of his 70th birthday. This work was supported by the CNRS and the Ministère de la Recherche. W.S. is grateful to the Fonds zur Förderung der wissenschaftlichen Forschung (FWF, Austria) for a postdoctoral grant (Erwin-Schrödinger-Stipendium Project No. J2021). Quantum chemical calculations have been carried out at the IDRIS computer center (Orsay, France) through a grant of computing time from CNRS. M.B. and M.-M.R. acknowledge support from the GdR DFT.

Supporting Information Available: X-ray crystallographic data for structure determination of **5**·C_6H_6 in CIF format. Atomic parameters used for the extended Hückel calculations (Table S1) and total energies and Cartesian coordinates for the optimal geometries (DFT/BP86) and an ORTEP view of the structure of **5** in **5**·C_6H_6 with the complete numbering scheme (Figure S1). This material is available free of charge via the Internet at http://pubs.acs.org. The crystallographic material can be obtained from the Cambridge Crystallographic Data Centre, 12 Union Road, Cambridge CB2 1EZ, UK (Fax: (44) 1223-336-033. E-mail: deposit@ccdc.cam.ac.uk), deposition number CCDC 265513.

JA051389Z

(33) (a) Sheldrick, G. M. *SHELXS-97: program for crystal structure solution*; Universität Göttingen: Germany, 1997. (b) Sheldrick, G. M. *SHELXL-97: program for refinement of crystal structures*; Universität Göttingen: Germany, 1997.